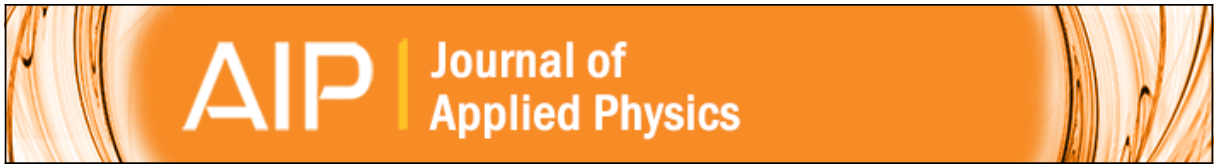

Nanostructure and giant Hall effect in TM x (Si O 2) 1 x (TM = Co , Fe , Ni) granular system

L. M. Socolovsky, C. L. P. Oliveira, J. C. Denardin, M. Knobel, and I. L. Torriani

Citation: Journal of Applied Physics **99**, 08C511 (2006); doi: 10.1063/1.2171013

View online: http://dx.doi.org/10.1063/1.2171013

View Table of Contents: http://scitation.aip.org/content/aip/journal/jap/99/8?ver=pdfcov

Published by the AIP Publishing

Nanostructure and giant Hall effect in $TM_x(SiO_2)_{1-x}$ (TM=Co,Fe,Ni) granular system

L. M. Socolovsky,[a] C. L. P. Oliveira,[b] J. C. Denardin, M. Knobel, and I. L. Torriani[b]
Instituto de Física Gleb Wataghin, UNICAMP, C.P. 6165, 13083-970 Campinas, SP, Brazil

(Presented on 31 October 2005; published online 21 April 2006)

Granular $TM_x(SiO_2)_{1-x}$ (TM=Co,Fe,Ni) thin films were thermally treated at different temperatures and their magnetotransport and structural properties were studied. Hall resistivity decreases with thermal annealing. Structure was analyzed based on small angle x-ray scattering results. A model of polydisperse system of hard spheres was used for obtaining structural parameters. Analysis reveals that a volume fraction of transition-metal atoms (less than 29%) are forming nanospheres. Changes in giant Hall effect upon annealing can depend on a particular combination of nanoparticle diameter, interparticle distance, and size distribution. © *2006 American Institute of Physics*.
[DOI: 10.1063/1.2171013]

Granular nanosized magnetic materials have unique properties that have atracted much attention in the last decades. One of these properties is the giant Hall effect (GHE), which appears in granular metal–dielectric systems.[1,2] In ferromagnetic materials two contributions to the Hall effect coexist: the ordinary Hall resistivity, which appears as a consequence of Lorentz force; and the extraordinary one, which is due to the spin-orbit interaction.[3] In granular systems, near the metal–insulator transition concentration both Hall resistivities show very large values, sometimes orders of magnitude larger than the value of the corresponding pure metallic sample.[1,2,4] The GHE decreases for higher metal concentrations.[2] Since the discovery of GHE, several experimental investigations have contributed to the understanding of the phenomenon with systematic studies in different granular metals.[2,4–6] Corresponding theoretical models have also been introduced.[7] Nevertheless, a model for GHE in magnetic systems has been elusive. A common feature of the films produced by co-sputtering, which is believed to be associated with GHE, is an extremely fine dispersion of metal particles embedded in the insulating matrix close to metal–insulator transition.[2,4,5] In order to develop a model for GHE it is necessary to obtain a reliable structural characterization of the nanostructured system. Sometimes it is hard to obtain a consistent histogram using transmission electron microscopy (TEM) images systems because the micrographs obtained represent projections of a three-dimensional system onto a plane. In addition, the statistics of the histograms are usually poor due to the limited particle count, generally limited to a few thousand particles in a typical area of 10^{-7} mm^2. On the other hand, small angle x-ray scattering (SAXS) can provide values that represent the scattering of a large number of particles ($\sim 10^{16}$/mm^3). SAXS samples do not require specific treatment for the measurements, while in TEM experiments small changes can be induced because of sample preparation (polishing, dimpling, ion bombardment).

In order to study the influence of the nanostructure on the magnetotransport properties of these granular materials, we have annealed $TM_x(SiO_2)_{1-x}$ (TM=Co,Fe,Ni) granular films at different temperatures between 150 and 400 °C, and fully characterized their structure by SAXS.

Thin films made by cosputtering of metal and SiO_2 were produced to have a metal concentration equal to or slightly higher than the percolation threshold, $x \sim 50\%$. Preparation details can be found in Ref. 2. Films of $Fe_x(SiO_2)_{1-x}$ $Co_x(SiO_2)_{1-x}$, $Ni_x(SiO_2)_{1-x}$, were deposited on glass and Kapton substrates. Hall resistivity was measured using the four-point method with a homemade system, in fields up to 2 T. Samples showing high extraordinary Hall resistivity (For Fe, $x=0.58$; for Co, $x=0.52$, and for Ni $x=0.56$) where chosen for this study. They were cut into pieces, and each one was thermally treated at $T_a=150$, 200, 250, 300, 350 and 400 °C, respectively. Annealing was done in a sealed oven, in a vacuum better than 10^{-6} Torr. The thermal treatment was performed using a fast heating rate, up to the desired temperature, then keeping the temperature constant for 15 min and subsequently applying a fast cooling rate. Samples prepared for SAXS measurements were deposited on Kapton films. These experiments were performed at the SAXS Beamline of the National Synchrotron Light Laboratory (LNLS, Campinas, Brazil). Transmission mode was used, with a wavelength of $\lambda=1.756$ Å. A camera length of 60 cm allowed us to measure SAXS intensity in a scattering vector range of $0.01291 \leqslant q \leqslant 0.49263$ Å^{-1}.

Figure 1 shows the absolute values of the room temperature extraordinary Hall resistivity ρ_{xys} as a function of annealed temperature for the samples studied. It can be observed that for the Co–SiO_2 sample ρ_{xys} increases from a value of 60.5 $\mu\Omega$ cm for the as-prepared sample up to 130 $\mu\Omega$ cm for a sample annealed at 250 °C, and then it decreases for the samples annealed above this temperature, down to 11 $\mu\Omega$ cm for 400 °C. A similar behavior is observed for both Ni–SiO_2 and Fe–SiO_2 samples. However, in such samples the increase in ρ_{xys} for low annealing tempera-

[a]Author to whom correspondence should be addressed; electronic mail: leandros@ifi.unicamp.br
[b]Also at: Laboratório Nacional de Luz Síncrotron, 13084-971 Campinas, SP, Brazil.

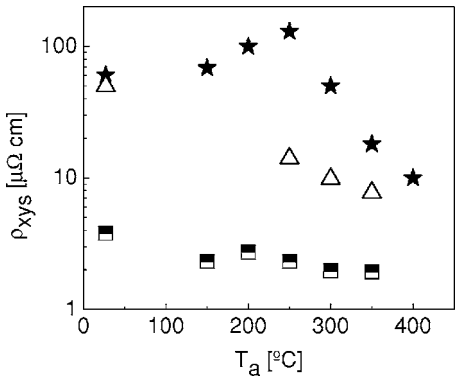

FIG. 1. Extraordinary Hall resistivity ρ_{xys} vs annealing temperature T_a for $Co_{52}-(SiO_2)_{48}$ (stars), $Ni_{56}-(SiO_2)_{48}$ (triangles), and $Fe_{58}-(SiO_2)_{42}$ (squares) samples.

tures was not detected, and only a suppression of the GHE upon annealing can be seen.

The dominant type of conductance in the samples can be determined from the analysis of the temperature dependence of resistivity, as shown in Fig. 2 for the annealed $Co-SiO_2$ sample. The temperature dependence of resistivity clearly shows an evolution with annealing temperature. For the as-prepared sample the dependence is approximately logarithmic, $\rho \propto -\log T$, with negative temperature coefficient of resistivity (TCR) in the whole scanned temperature range. A similar temperature dependence of resistivity has been observed in other cosputtered metal–insulator materials that also present an enhanced GHE.[1,2,4,5] It is worth noting that the samples annealed up to 250 °C, which present an increase in the giant Hall resistivity (see Fig. 1), keep the negative TCR and the $-\log T$ dependence in the whole temperature range. This result is in perfect agreement with those observed before,[5] and corroborates the association between GHE and a large resistivity with a $-\log T$ dependence. Upon annealing at higher temperatures the Hall resistivity decreases, accompanied by the appearance of a positive TCR in the resistivity versus temperature curves near room temperature, when the samples start to display a metallic character.

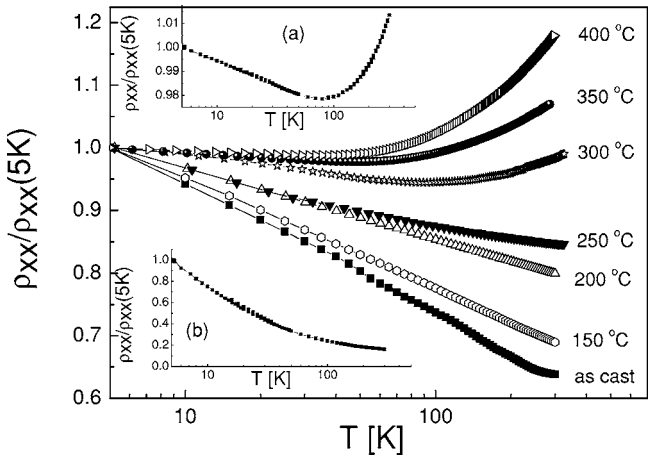

FIG. 2. Resistivity, normalized to the values at $T=5$ K, as a function of the logarithm of temperature for the as cast $Co-SiO_2$ sample and the ones annealed up to different temperatures T_a. (Inset) The curves for as -prepared (a) $Fe-SiO_2$ and (b) $Ni-SiO_2$.

The temperature dependencies of resistivity for the $Ni-SiO_2$ and $Fe-SiO_2$ as-prepared samples are shown in the insets of Fig. 2. The curve of the $Fe-SiO_2$ sample displays a negative TCR at low temperatures (for $T<70$ K) and a positive TCR close to room temperature. This trend can be related to the observed continuous decrease of the Hall effect upon annealing for this particular sample (see Fig. 1). The behavior of the $Ni-SiO_2$ curve is similar to that of the $Fe-SiO_2$ sample. At $T=16$ K it departs from a $-\log T$ law. Despite the fact that the metallic concentration is larger than in the $Co-SiO_2$ sample, the $Ni-SiO_2$ sample is more insulating, and the Hall resistivity could not be measured for all annealed samples due to parasitic magnetoresistance.

In order to investigate the mechanism behind the observed changes in the Hall effect and resistivity upon annealing, SAXS experiments were performed.

SAXS spectra show features typical of polydisperse systems.[8] One of its features, a maximum located at $q=0.1-0.2$ Å^{-1} (Fig. 5 of Ref. 8) is atributed to spatial correlation effects coming from nanoparticle interaction. TEM images showed the existence of spherical nanosized particles.[8] Due to the high volume fraction, it is necessary to take into account the structure factor for the analysis of the curves. A model for describing SAXS intensity that takes into account both particle form factors P and system structure factors S was used to analyze the measured spectra.[9–11]

$$I(q) = \int_V \eta \,.\, P(q,R,\Delta R,\Delta\rho) \,.\, S(q,R_{HS}) dR,$$

where η is the nanoparticle volume fraction. P takes into account the fact that the system is polydisperse, formed by spherical particles with radius R, following a Gaussian distribution, characterized by a mean radius $\langle R\rangle$ and a width σ. $\Delta\rho$ is the electron density contrast between nanoparticles and matrix. Calculations of S were made in terms of a hard-sphere model, characterized by a mean interaction radius R_{HS}. A detailed explanation of the use of this model and its application to the analysis of $Co-SiO_2$ samples is given elsewhere.[11] Several fittings using different values of η were done for each spectrum. The value of η that minimizes χ is always less than 0.29. This indicates that this fraction is the maximum amount of metallic atoms that are in form of nanoparticles. The remaining fraction of metallic atoms present in the samples may contribute to the formation of very large clusters, whose presence is considered to be responsible for the sharp rise of the intensity values in the small q region. Curve fittings are good in all cases. Fitting results are plotted as a function of the thermal treatment temperature T_a in Fig. 3. It can be seen that when T_a increases, $\langle R\rangle$ increases for cobalt samples, and oscillates for the other two samples. For Fe and Ni samples, initially $\langle R\rangle$ decreases and then it increases for $T_a \geqslant 200$ °C. The final size is almost the same for the three samples, $\langle R\rangle = 2.1$ nm. Mean interaction radius R_{HS} decreases monotonically for Co samples, and oscillates for Fe and Ni. The volume distribution width is never bigger than 1.55 nm. The volumetric fraction varies between 0.205 and 0.29. For the highest T_a the value falls to values less than

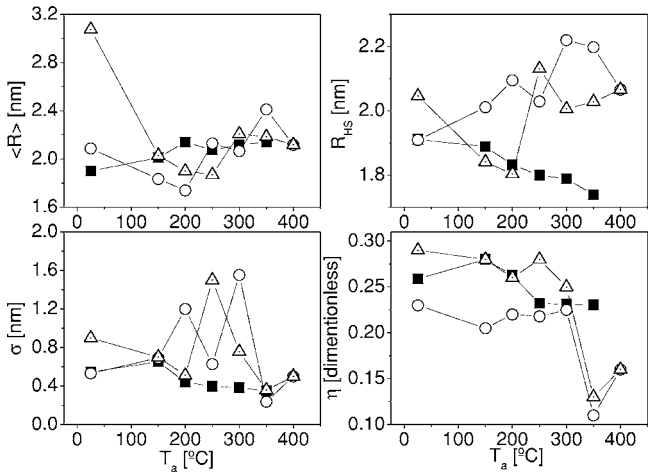

FIG. 3. Fitted SAXS parameters for different annealing temperatures. Data for $Co_{48}(SiO_2)_{52}$ (black squares), $Fe_{58}(SiO_2)_{42}$ (open circles), and $Ni_{56}(SiO_2)_{44}$ (open triangles).

0.16 for Fe and Ni samples, indicating that part of the former nanoparticles coalesced into larger structures.

As mentioned above, thermal treatment induces rather intricate changes on the nanostructure of the three as-prepared samples. If one considers the involved diffusion processes, different mechanisms for diverse situations (such as isolated metal atoms in the SiO_2 matrix, metal atoms in the vicinity of nanoparticles, nanoparticles touching to each other, etc), must be taken into account, and each one of them causes different effects on the physical properties, in particular the magnetotransport processes. Considering the behavior of the GHE for each group of samples it is seen that only one structural parameter cannot explain the observed changes upon annealing. If the GHE property is attached to only one of the structural parameters, a decrease (or increase) in $\langle R \rangle$, R_{HS}, or σ could lead to a change of the Hall resistivity, a fact that is not observed. Taking into account that the original samples have similar metallic concentrations, it was expected that at the beginning the effect of the thermal annealing on the structure would be the same for all the samples studied. However, the experimental data indicates that even small initial differences lead to different nanostructures and, consequently, to different Hall resistivities upon annealing. Therefore, the changes observed in the GHE for different nanostructures (as a result of the thermal treatments) is due to a subtle combination of values of $\langle R \rangle$, R_{HS}, and σ. More experiments are currently being performed in order to better understand the complex relationship between the nanostructure and the Hall resistivity.

The Brazilian agencies Fundação de Amparo à Pesquisa do Estado de São Paulo (FAPESP), Conselho Nacional de Desenvolvimento Científico e Tecnológico (CNPq); and Synchrotron Light National Laboratory (LNLS, Campinas, Brazil—for the use of SAS line) are acknowledged. X.X. Zhang is acknowledged for the samples.

[1] A. B. Pakhomov, X. Yan, and B. Zhao, Appl. Phys. Lett. **67**, 3497 (1995).
[2] J. C. Denardin, M. Knobel, X. X. Zhang, and A. B. Pakhomov, J. Magn. Magn. Mater. **262**, 15 (2003).
[3] C. M. Hurd, *The Hall Effect in Metals and Alloys* (Plenum, New York, 1972).
[4] X. X. Zhang, C. Wan, H. Liu, Z. Q. Li, P. Sheng, and J. J. Lin, Phys. Rev. Lett. **86**, 5562 (2001).
[5] X. N. Jing, N. Wang, A. B. Pakhomov, K. K. Fung, and X. Yan, Phys. Rev. B **53**, 14032 (1996).
[6] B. A. Aronzon, A. B. Granovskii, D. Y. Kovalev, E. Z. Meilikhov, V. V. Ryl'kov, and M. V. Sedova, JETP Lett. **71**, 469 (2000).
[7] C. C. Wan and P. Sheng, Phys. Rev. B **66**, 075309 (2002).
[8] L. M. Socolovsky, J. C. Denardin, A. L. Brandl, and M. Knobel, Mater. Charact. **50**, 117 (2003).
[9] C. Robertus, W. H. Philipse, J. G. H. Joosten, and Y. K. Levine, J. Chem. Phys. **90**, 4482 (1989).
[10] D. I. Svergun, P. V. Konarev, V. V. Volkov, M. H. J. Koch, W. F. C. Sager, J. Smeets, and E. M. Blokhuis, J. Chem. Phys. **113**, 1651 (2000).
[11] L. M. Socolovsky, C. L. P. Oliveira, J. C. Denardin, M. Knobel, and I. Torriani, Phys. Rev. B **72**, 184423 (2005).